Mycobacterium tuberculosis Rv3194c efficiently facilitates mycobacterial-lung epithelial interaction through its HA-binding site

Dongyue Zhao*, Chen Xu, Danfeng Lin*

Fujian Key Laboratory of Developmental and Neurobiology, College of Life Science, Fujian Normal University, Fuzhou 350117, Fujian Province, China

Running title: Rv3194c was identified as a novel adhesin

*To whom correspondence should be addressed:

Dongyue Zhao, Fujian Key Laboratory of Developmental and Neurobiology, College of Life Science, Fujian Normal University, Qishan Campus, No.1 Keji Road, Fuzhou, Fujian, China 350117. Email: mountain@fjnu.edu.cn

Danfeng Lin, College of Life Science, Fujian Normal University, Qishan Campus, No.1 Keji Road, Fuzhou, Fujian, China 350117. Email: 75562865@qq.com

Abstract: *Mycobacterium tuberculosis* adhesins are surface-exposed molecules that mediate pathogen-host interaction, a fundamental step towards host infection. Here we show that serine protease (Rv3194c) promotes mycobacterial infection to lung epithelial through its hyaluronic acid (HA)-binding site. Both enzyme-linked immunosorbent assay and surface plasmon resonance analysis revealed that Rv3194c bound to HA. Utilizing synthetic peptides, we next defined HA-binding site of 20 amino acids from 91 to 110 of Rv3194c (P91-110). Immunofluorescence assay and an FACScan showed that Rv3194c was interacted with A549 cells (human lung epithelial cells), and its interaction was abolished by the addition of

hyaluronidase or P91-110. Experimental infection *in Vitro* revealed that Rv3194c participates in attachment of recombinant *Mycobacterium smegmatis* (Rv3194c/MS) to A549 cells, and P91-110 treatment of A549 cells almost inhibited Rv3194c/MS-A549 cells interaction. To provide *in vivo* evidence, we constructed a reporter strain of *M. smegmatis* expressed a derivative of the firefly luciferase that is shifted to red (FFlucRT) in combination with Rv3194c (Rv3194c+FFlucRT/MS) to infect the rodents and monitor the progression of the disease. Using bioluminescence imaging and bacterial counts in lung tissue confirmed that Rv3194c dramatically enhanced the persistence of *M. smegmatis*. In addition, treatment of intratracheal Rv3194c+FFlucRT/MS-infected mice with P91-110 significantly suppressed the growth of Rv3194c+FFlucRT/MS *in vivo*. Taken together, these results demonstrate that Rv3194c was identified as a novel adhesin, and P91-110 has potential for therapeutic and prophylactic interventions in mycobacterial infection.

Key words: *Mycobacterium tuberculosis*, adhesion, host-pathogen interaction, surface plasmon resonance, bioluminescence imaging

Tuberculosis (TB) caused by *M. tuberculosis* is primarily a respiratory disease that results in chronic consumption (1). It has been clearly shown that *M. tuberculosis* interacts with host cells and enters them (2). Such cells include epithelial cells, macrophages and dendritic cells during the infection process (3). This process of entry into the host cells is critical to activate the associated virulence factors (4). In addition, this process of attachment improves the pathogen's ability to spread and to avoid the host's immune response (5). The binding of adhesins to extracellular matrix (ECM) components or trans-membrane proteins is main ways to bacteria to

attach to the surface of their host (6). These adhesins bound to the extracellular matrix (ECM) compounds including collagens, bone sialoprotein, fibronectin, elastin, laminin, glycosaminoglycans (GAGs) and vitronectin (7). Because they have a central role in the interaction of pathogen with host, pathogenic bacteria have evolved a sizeable diversity of factors that mediate adherence (8). Pili are a surface structure similar to hair, and their distal tip contains an adhesin; their function in adhesion has been deciphered (9). However, Bacteria have also been found to contain a large of adhesins that do not involve pili. The Pro-Glu (PE) polymorphic GC-rich repetitive sequence (PGRS) (10) protein encoded by *Rv1818c* and the curli pili (MTP) (10, 11) encoded by *Rv3312A* play key roles in the ability of *M. tuberculosis* to adhere to epithelial or macrophage cells. Hickey et al. (12) showed that *M. tuberculosis* DnaK and Cpn60.2 are found on the surface of the bacteria, and Cpn60.2 facilitates the effective association between the bacteria and macrophages. Kumar et al. (13) used an ELISA (image-based enzyme-linked immunosorbent assay) technique to prove that the recombinant Rv2599, Rv3717 and Rv0309 protein could bind the ECM component. Pethe et al. (14) showed that the laminin binding protein produced by *M. smegmatis,* which *M. tuberculosis* also expresses, binds to laminin. Kinhikar et al. (15), Espitia et al. (16) and Xolalpa et al. (17) found that the fractionated recombinant Rv1759c, PE-PGRS protein and glutamine synthetase A1 bound to fibronectin. Esparza et al. (18) and Diaz-Silvestre et al. (19) discovered that PstS-1 (the *M. tuberculosis* 38 kDa glycoprotein) and LpqH glycolipoprotein (the 19 kDa antigen) act as an adhesin that can bind the mannose receptor and promote the phagocytosis of the mycobacteria. Mycobacterial DNA binding protein 1 (MDP-1) (20) and heparin-binding hemagglutinin (HBHA)

(21) in *M. tuberculosis* are key factors involved in the adherence to lung epithelial cells by binding HA. Therefore, the more thorough understanding of the interaction is essential to develop prophylactic/therapeutic strategies against tuberculosis.

The interaction with the epithelia is considered to be critical to enable the bacteria to disseminate and dominate the outcome of the disease (22). In addition to the adhesins described above, *M. tuberculosis* may have the other adhesins. Analysis of Rv3194c using the SMART tool (http://smart.embl-heidelberg.de/) has shown that 123-192 amino acids are a PDZ domain, 131-194 are an SCOP (Structure Classification of Proteins, http://scop.mrc-lmb.cam.ac.uk/scop/data/scop.b.html) domain, d1g9oa_, of which the members might possess the capacity of binding DNA, ATP or proteins associated with apoptosis and 232-330 are a Lon C domain. In addition, the minimal HA-binding requirement ($_{94}$**R**DLVYPPG**K**$_{102}$), the B(X_7)B motif (23), was found in the sequence of Rv3194c, which might possess adhesion characteristics. The recent study (24) demonstrated that Lon C domain in Rv3194c hydrolyzes BSA, casein, gelatin, and milk, and degraded the complement components, C3b and C5a. However, the ligands that PDZ domain binds to have been unidentified, and whether its B(X_7)B (23) motif possesses adhesion characteristics has not been known. Therefore, our works focus on the adhesion role of the extracellular Rv3194c. The results indicate that Rv3194c mediates the mycobacteria-lung epithelial interactions through binding of peptide corresponding to an amino acid sequence of Rv3194c at the 91-110 position (P91-110), HA-binding site, to HA in cell surface. In addition, the growth of recombinant *M. smegmatis* (rMs) *in vivo* was notably reduced when the mice was treated with P91-110. In summary, the

Rv3194c acts as a novel adhesin, and its peptide, P91-110, may be a candidate drug against tuberculosis.

Results

Expression and purification of the Rv3194c protein

To obtain the potential structural information of the Rv3194c protein, we first examined its sequence with several types of structure prediction software. TMHMM server (http://www.cbs.dtu.dk/services/TMHMM-2.0/) predicted a transmembrane helix from 1 to 27. Because the hydrophobic sequence from the trans-membrane domain might make the protein more difficult to express, *Rv3194c* without the trans-membrane helix sequence was cloned into a His-tag vector to produce a His-tagged fusion protein. To facilitate the activity of the target protein and to increase the amount of the soluble fraction, the expression condition with 0.5 mM IPTG at 23°C for 12 h was optimized. After ultra-sonication, the soluble protein in the supernatant was purified by affinity chromatography with Ni^{2+}. After purification, the recombinant Rv3194c showed the expected molecular size (35 kDa) when analyzed using SDS-PAGE (**Fig. 1A**). A western blotting further revealed that an approximately 35 kDa protein band was the Rv3194c protein after it was probed with the anti-Rv3194c antisera (**Fig. 1B**). The 35 kDa protein from cell lysate of BCG, as the positive control, was recognized by anti-Rv3194c antisera (**Fig. 1B**). Followed by using the Superdex 75 gel chromatography methods for the protein's separation and purification, we have got the more than 99% protein of Rv3194c (**Fig. 1C**). Finally, mass spectrometry and peptide mass fingerprinting results confirmed that the expected protein, Rv3194c (Accession No. NP_217710.1), was obtained from H37Rv (**Fig. 1D**).

Determination of the HA-binding Site of Rv3194c

Analysis of Rv3194c revealed that the minimal HA-binding requirement ($_{94}$**R**DLVYPPG**K**$_{102}$), the B(X_7)B motif (23), was found in the sequence of Rv3194c, which might possess adhesion characteristics. To elucidate this hypothesis, we examined whether Rv3194c binds to HA. The ELISA showed that Rv3194c bound to HA, but not mannose, dextran and galactose (**Fig. 2A**); the Rv3295, as a negative control protein, does not bind to HA, dextran, mannose and galactose (**Fig. 2A**). To explore the role of extracellularly occurring Rv3194c, HA-Sepharose Chromatography was used to examine the binding capacity of Rv3194c to HA. HA-binding protein, Rv3194c protein on western blotting analysis, was eluted by PBS containing 1.5 M NaCl (**Fig. 2B**). To determine its binding site, we examined the HA-binding activity of 20-mer of synthetic peptides covering the entire sequence of Rv3194c. ELISA showed that the HA bound to the peptide corresponding to an amino acid sequence of Rv3194c at the 91-110 position (P91-110) (**Fig. 2C**). The results indicated that Rv3194c bound to HA through its P91-110.

SPR analysis of the interaction between Rv3194c and the HA

Based on results as described above, Rv3194c and P91-110 were respectively treated as an immobilized ligand in the following studies. To elucidate the molecular interaction, an SPR analysis was performed. Rv3194c, P91-110 and Rv3295 were immobilized on the CM5 sensor chip until they had gained 3253, 3212 and 3034 resonance units (RUs). HA (10 μg/mL) was injected into the immobilized cells with either Rv3194c or P91-110 for 30 s. As predicted from the analysis by HA-Sepharose Chromatography, the interaction of Rv3194c or P91-110 with HA

was observed until they had gained 85 RU or 110 RU, respectively (**Fig. 3A**). HA had no interactions with Rv3295 or the empty sensor (data not shown). The affinity (K_D) of HA bound to Rv3194c or P91-110 was 2×10^{-8} mol/L or 1.6×10^{-8} mol/L, respectively (**Fig. 3B**). The reason for the difference of K_D value, a part of the binding site of synthetic peptide may be masked during immobilization procedure. In contrast, different types of carbohydrates including mannose, dextrose and galactose, lacked the ability to bind to Rv3194c or Rv3295 (data not shown). The results of the SPR analysis indicate that Rv3194c bound to HA with highest affinity, and the P91-110, HA-binding Site, was also further confirmed (**Fig. 3**).

Rv3194c Binds to the A549 Human Lung Epithelial Cells

HA, a glycosaminoglycans (GAGs), located in the surface of Lung Epithelial Cells, possessing diverse biological functions. The results (**Figs. 2 and 3**) prompted us to examine the possibility that the Rv3194c may participate in the binding to A549 epithelial cells. Rv3194c and P91-110 conjugated with red fluorescent group known as Cy3 at its N-terminal (Cy3-P91-110) were respectively incubated with A549 cells to determine if they can bind to the epithelial cells. Confocal laser microscopy showed that Rv3194c and Cy3-P91-110 attached to the cells, but not that of Rv3295 (**Fig. 4A**). The binding of Cy3-P91-110 to A549 cells was obvious by 10 min, and by 1 hour after the addition, the binding had reached a plateau; More than 98% of the A549 cells were Cy3-P91-110-positive 1 h later (**Fig. 4B**). In contrast, binding of Rv3194c was delayed, and 20% of cells were Rv3194c negative even at the plateau phase, suggesting that the binding of P91-110 to cells is more efficient than that of Rv3194c (**Fig. 4B**). To determine whether the binding of Rv3194c to A549 cell relies on HA, the subsequent experiments were

conducted. We studied the ability of the exogenous hyaluronidase, HA or P91-110 to inhibit the reaction. FACScan showed that the percentage of binding of Rv3194c to untreated A549 cells was more than 98% (**Fig. 4C**); percentage of binding of Rv3194c to A549 cells pretreated with hyaluronidase, HA or P91-110 was respectively less than 5.2%, 51% or 3.2% (**Fig. 4C**), indicating that addition of exogenous hyaluronidase or P91-110 abolished Rv3194c-A549 cells interaction compared to that of added HA. In total, these findings indicated that Rv3194c bound to epithelial cells through its P91-110 interaction with HA in cells.

Rv3194c participates in the attachment of recombinant M. smegmatis to the A549 cells

BLAST analysis of nucleotide and amino acid sequences revealed that the *Rv3194c* exists in pathogenic mycobacteria: *M. tuberculosis, M. bovis* and *M. africanum*, but absent in non-pathogenic mycobacteria: *M. avium*, *M. smegmatis* and other non-tuberculous mycobacteria. Additionally, the nucleotide sequence of *Rv3194c* is highly conserved in pathogenic mycobacteria. To clarify the involvement of Rv3194c in the attachment and invasion by the mycobacteria, A549 cells were infected with recombinant *M. smegmatis* (Rv3194c/MS and pMV261/MS) *in vitro*. A549 cells attached by Rv3194c/MS were visualized by confocal laser microscopy, indicating that Rv3194c participates in binding of Rv3194c/MS to A549 cells (**Fig. 5A**). CFU-based analyses showed that bacterial counts of Rv3194c/MS in untreated group significant higher than that in HA or P91-110 pretreated group (**Fig. 5B**). Bacterial counts of Rv3194c/MS in P91-110 pretreated group was significantly lower than that of HA added group (**Fig. 5B**). These results demonstrated that Rv3194c participates in attachment of Rv3194c/MS to A549 cells, and P91-110 treatment of A549 cells almost inhibited Rv3194c/MS-A549 cells

interaction and addition of exogenous HA reduced the binding of Rv3194c/MS to A549 cells (**Fig. 5**). We next examined where Rv3194c in Rv3194c/MS was localized using western blotting analyses. The results demonstrated that the Rv3194c expressed in cell lysate, cell wall, cytoplasm and cell membrane (**Fig. 5C**). Rv3194c was detected in cell culture filtrates as well, indicating that the Rv3194c is a secreted protein (**Fig. 5C**).These data demonstrated that the Rv3194c is required when mycobacteria adheres its host cells.

Persistence in the lung of the recombinant M. smegmatis expressed Rv3194c

The epithelial cells are target cells for adherence and invasion by mycobacteria (25). Therefore, we expanded our *in vitro* experiments to examine animals *in vivo* to delineate the roles that the Rv3194c play in the mycobacterial/host interaction. To monitor the progression of disease in living animals using bioluminescence imaging, we constructed a reporter strain of *M. smegmatis* including Rv3194c+FFlucRT/MS and FFlucRT/MS (**Fig. 6A**). There was no significant difference among the four groups 1 day after infection (**Fig. 6B**). The bacterial loads were notably higher after infection with Rv3194c+FFlucRT/MS at 4, 7 and 14 days compared to other three groups (**Fig. 6B**). Bacterial loads in the lung tissues of FFlucRT/MS group were completely cleared 14 days after infection (**Fig. 6B**). Furthermore, bacterial loads in the lung tissues of the Rv3194c+FFlucRT/MS plus of P91-110 group were significantly lower than that in Rv3194c+FFlucRT/MS plus of HA group at 7 days and almost cleared at 14 days (**Fig. 6B**). Images of the infected mice were captured at multiple time points after the administration of intraperitoneal luciferin. Imaging mice that had been inoculated with *M. smegmatis* were used to estimate the bioluminescence background level (**Fig. 6C**). The live mice were subjected to *in*

190 *vivo* imaging, and bioluminescence levels were no significant difference among the four groups 1
191 day after infection (**Fig. 6C**). Bioluminescence levels in the lung tissues of
192 Rv3194c+FFlucRT/MS group were significantly higher than that in other three groups at 4, 7 and
193 14 days (**Fig. 6C**). Bioluminescence levels in the lung tissues of Rv3194c+FFlucRT/MS plus of
194 P91-110 group was significantly lower than that in added HA group at 14 days and was close to
195 background level (**Fig. 6C**). Using bioluminescence imaging and bacterial counts confirmed that
196 Rv3194c enhanced the persistence of *M. smegmatis*, and P91-110 more efficiently prevents mice
197 to be infected with Rv3194c+FFlucRT/MS (**Figs. 6B, C**). As expected, there was a strong
198 correlation between the bioluminescence in the thorax of the live mice and CFU in the lungs.
199 These findings demonstrated that Rv3194c serves as a novel adhesin, and P91-110 efficiently
200 suppress the growth of mycobacteria *in vivo* and may be a candidate drug against tuberculosis.
201

202 **Discussion**

203 Anti-adhesion therapy represents a potentially promising avenue for the treatment and prevention
204 of tuberculosis in a post-antibiotic era (26). Adhesins are surface-exposed microbial structures or
205 molecules that enable pathogenic organisms to adhere to host surfaces, a fundamental step
206 towards host infection (27). The Rv3194c protein belongs to the S16 serine protease family.
207 Analysis of sequence has shown that 1-23 amino acids are a potential signal peptide and 1-27
208 amino acids are a trans-membrane helix. Moreover, the *Rv3194c* gene exists only in pathogenic
209 mycobacteria including *M. tuberculosis*, *M. africanum*, and *M. bovis*. Therefore, the protein is
210 hypothesized to be associated with mycobacterial pathogenesis. To verify this hypothesis, we

211 performed the following studies. Our focus was on the physiological role of the extracellular
212 Rv3194c. Based on the B(X_7)B motif in this protein, we hypothesized that Rv3194c acts as an
213 adhesin in the mycobacterial/epithelial cell interaction. In our research, we explored the
214 interaction of Rv3194c with HA (**Figs. 2A, B**). Utilizing synthetic peptides, we next defined the
215 peptide corresponding to an amino acid sequence of Rv3194c at the 91-110 position (P91-110) is
216 responsible for the specific HA-binding site of Rv3194c (**Fig. 2C**). Their affinity was determined
217 using SPR analysis (**Fig. 3**). The surface HA of A549 cells, as the primary receptor, was
218 recognized by P91-110 (**Fig. 4**). Treatment with P91-110 significantly inhibited the
219 mycobacterial binding to the A549 cells compared to that of HA (**Figs. 5B**). The manner by
220 which Rv3194c is expressed in the mycobacterial cell wall, cytoplasm and cell membrane in
221 Rv3194c/MS was discovered (**Fig. 5C**). To our knowledge, this is the first study to demonstrate
222 that a bacterial pathogen utilizes Rv3194c to attach to its host cells. Given our findings from the
223 *in vitro* experiments, we attempted to therapeutically intervene with infection in a murine model.
224 The treatment of such mice with P91-110 produced a striking decrease of *M. smegmatis*
225 expressing Rv3194c in the lung (**Fig. 6B**). These findings back up the *in vitro* experiments that
226 found that Rv3194c participates in the mycobacterial/lung epithelial cell interaction. To further
227 confirm its role in adhesion, we constructed a reporter strain of *M. smegmatis* which expressed
228 firefly luciferase and Rv3194c to monitor the progression of the disease in the living animals.
229 The bioluminescence imaging in the lung tissue further confirmed that Rv3194c is required for
230 infection, because the persistent ability of recombinant *M. smegmatis* was considerably enhanced
231 compared to that of the parent strain (**Fig. 6C**). In addition, growth and bioluminescence levels

of reporter strain that expressed Rv3194c was marked reduced when the mice was treated with exogenous P91-110 (**Figs. 6B, C**). In this study, Rv3194c was identified as a novel adhesin and was a promising drug target against tuberculosis.

Materials and methods

Cloning, expression and purification

The *Rv3194c* coding sequence without the predicted transmembrane fragment was amplified from *M. tuberculosis H37Rv* genomic DNA using the following primers: the sense primer *Rv3194c*-F: 5'-TAT**CATATG**CCGTTTGTGGCGCTGG-3', containing an *Nde* I digestible site; the antisense primer *Rv3194c*-R: 5'-GGT**GAATTC**CTAGCAGCTCGGCGTCG-3', including an *Eco*R I site. PrimeSTAR Max DNA polymerase from TaKaRa Bio (Otsu, Japan) was used to amplify the PCR. The *Rv3194c* amplicon was cloned into a pET28a (+) vector (Novagen, Darmstadt, Germany) that had a 6×His-tag at its N-terminus. The recombinant plasmid pET-28a-*Rv3194c* was then transformed into *E.coli* (BL21) cells. A signal clone was selected and grown in LB media (200 μg/mL ampicillin and 34 μg/mL chloromycetin) at 37 °C overnight. The overnight culture was inoculated into fresh LB medium with kanamycin (50 μg/mL) until their OD_{600} reached 0.6 to 1.0. At that point, they were induced to express the protein by induction with isopropylβ-$_D$-1-thiogalactopyranoside (IPTG) at a concentration of 0.5 mM at 23 °C for 12 h. Affinity chromatography using Ni Sepharose 6 Fast Flow (GE Healthcare Life Sciences, Little Chalfont, United Kingdom) was used to purify the protein as previously described (28). The purified protein was centrifuged by a 20 kDa-cut-off membranes made by Millipore (Milford,

253 MA, USA) until the volume was approximately 1 mL. The concentrated protein was then loaded
254 onto superdex75 (10/60) chromatography column (GE Healthcare) pre-equilibrated with 20 mM
255 Tris-HCl buffer at pH 7.4. The desired protein was then eluted by 200 mM NaCl in Tris-HCl
256 buffer at pH 7.4. A flow rate of 1 ml/min was maintained, and 2 ml of each tube was collected.
257 The eluted fractions were collected and analyzed by SDS-PAGE. Finally, Rv3194c was
258 completely identified by mass spectrometry as previously described (29).

259 ***Construction of the FFlucRT reporter strains and polyclonal anti-Rv3194c sera***

260 We used the pMV306DIG13+*FFlucRT* (addgene Plasmid #49998) as a PCR template to
261 amplify the G13 promoter and the *FFlucRT* gene fragment using the following primers: the sense
262 primer: 5'-**AAGCTT**GCAGCCGAACGACCGA-3' containing a *Hind* III digestible site; the
263 antisense primer: 5'-**GTCGAC**TCTAGATCACAATTTCGA-3' containing a *Sal* I digestible site.
264 The underlined sections indicate the restriction sites. A *Hind* III-*Sal* I 2.179-kbp fragment
265 containing the G13 promoter sequence and the gene that encodes FFlucRT was cloned into an *E.*
266 *coli-mycobacterium* shuttle vector pMV261 to produce the plasmid pMV261-*FFlucRT*. To obtain
267 pMV261-*FFlucRT-Rv3194c*, *Rv3194c* coding sequence including the predicted transmembrane
268 helices was amplified using the following primers: the sense primer *Rv3194c*-F:
269 5'-**TTCGAA**GTGAATAGGCGGATATTGACC-3', containing an *Bst*B I digestible site; the
270 antisense primer: *Rv3194c*-R: 5'-**AAGCTT**CTAGCAG CTCGGCGTCG-3', including a *Hind* III
271 digestible site, and then was cloned into plasmid pMV261-*FFlucRT* by its digestible sites. The
272 rMS (Rv3194c+FFlucRT/MS, FFlucRT/MS, Rv3194c/MS and pMV261/MS) was constructed by
273 the electroporation of *M. smegmatis* with the equivalent vector. The rMS was grown in 7H9

broth at 37 °C until the OD_{600} was 0.8 to 1.0. 1 mg of Rv3194c emulsified in incomplete Freund's adjuvant was injected multiple times (0, 20 and 40 days) into female rabbits to produce polyclonal anti-Rv3194c sera. Sera were collected as previously described (30). The polyclonal anti-Rv3194c antibody was obtained as previously described (30).

Preparation of the subcellular fractions of the rMS

To obtain the rMS subcellular fractions, all the subsequent procedures were conducted at 4°C. The rMS cells were resuspended in proteinase inhibitor cocktail, sonicated for 15 min on an ice bath, let to settle for 15 min and again sonicated same as before. The unbroken cells were removed by centrifugation at 3,000 *g* for 5 min. The supernatant and the pellet from supersonic lysate were respectively collected by centrifugation at 27,000 *g* for 1 h. The pellet was resuspended in lysis buffer plus1mM PMSF and centrifuged one time at 27,000 *g* for 1 h. The pellet from this centrifugation was resuspended in 10 mM ammonium bicarbonate. This preparation served as the cell wall fraction. The resultant supernatant (the first and second centrifugations at 27,000 *g*) were pooled and centrifuged at 100,000 *g* for 4 h. After centrifugation, the supernatant and pellet were respectively used as the cytoplasmic and membrane-ribosome fractions. Each fraction was tested with polyclonal antibodies against Rv3194c. The results were detected and recorded using a Li-Cor Odyssey imaging system (Li-Cor Biosciences, USA)

Detection of the binding of Rv3194c to the HA using enzyme-linked immunosorbent assays

HA, Dextran, Mannose and galactose were respectively immobilized on a 96-well ELISA plate manufactured by Sumitomo (Osaka, Japan) at a concentration of 100 μg/mL in carbonate

295 buffer, pH 7.4, overnight at 4 °C. Following the blockage of the wells with 5% BSA in PBS, 10
296 μg/mL of Rv3194c in PBS that contained 0.05% Tween 20 (PBS-T) was added to each well and
297 incubated for 1 h at 37 °C. After three washes, anti-Rv3194c antisera diluted 1:1000 in PBS-T
298 was added and incubated for 2 h at 37 °C. After three washes, anti-rabbit IgG antibody
299 conjugated with peroxidase (1:10000) was added and incubated for 1 h at 37 °C. Following three
300 washes, 3',5,5'-tetramethylbenzidine (TMB), as Chromogenic substrate, was added and
301 incubated for 10 min at 37 °C. A stop solution was utilized to cease the enzymatic chromogenic
302 reaction, and then optical density was read at 630 nm.

303 ***HA-Sepharose Chromatography***

304 100μg of Rv3194c in PBS containing 0.15 M NaCl were applied to HA-Sepharose
305 chromatography (Amersham Biosciences) as previously described (31). The unbound proteins
306 were removed by washing the gel with PBS containing 0.15 M NaCl. The bound proteins were
307 eluted by PBS containing 1.5 M NaCl. A flow rate of 1 ml/min was maintained, and 1 ml of each
308 fraction was collected. The fraction was analyzed by Western-blotting.

309 ***Determination of the HA-binding site by ELISA***

310 20-mer of synthetic sequential peptides corresponding to the amino acid sequence of
311 Rv3194c were immobilized on the 96-well ELISA plate (Sumitomo, Osaka, Japan) at a
312 concentration of 10 μg/mL in carbonate buffer, pH 9.6, overnight at 4 °C. After blocking the
313 wells by 5% BSA in PBS, 100 μg/ml of biotinylated HA (Sigma) was added to each well and
314 incubated for 1 h at 37 °C. After washing unbound HA, horseradish peroxidase-conjugated
315 streptavidin was added, and the mixture was incubated for 1 h at 37 °C. After washing free

316 streptavidin, binding was detected by color development with *o*-phenylendiamine
317 dihydrochloride (Wako, Tokyo, Japan), and ELISA units (optical density) were measured at 490
318 nm.

319 ***Surface Plasmon Resonance Measurements***

320 The interaction of Rv3194c or peptide corresponding to an amino acid sequence of
321 Rv3194c at the 91-110 position (P91-110) with HA was monitored by determining the SPR using
322 a BIAcore 2000 biosensor (Uppsala, Sweden). All the reactions were conducted in binding buffer
323 (10 mM HEPES, 0.005% P20 surfactant, 3 mM EDTA and 150 mM NaCl), at 25 °C. The
324 Rv3194c and P91-110 were immobilized on a BIAcore CM5 sensor chip using an amine
325 coupling kit as described by the manufacturer. The calculation of the association and dissociation
326 rate constants was conducted by nonlinear fitting of the primary sensorgram data using version
327 3.0 of BIAevaluation software.

328 ***Protein binding assay for the A549 type II human lung epithelial cells***

329 A549 cells were cultured in complete culture media (RPMI 1640 media, 10% fetal bovine
330 serum, 2 mM L-glutamine, 5.5×10^{-5} M 2-mercaptoethanol and 25 mM HEPES). 10×10^{5}
331 cells/mL was allotted into individual wells of a 6-well plate (BD Biosciences) and incubated in a
332 humidified atmosphere that contained 5% CO_2 for 24 h at 37°C. After twice washes with RPMI
333 1640 media and refilling the volume with 1mL of complete culture media, cells were treated with
334 100 μg/mL of hyaluronidase, HA or P91-110 for 2 h. The untreated cells and treated cells were
335 respectively incubated with Rv3194c for 1h. After incubation, the wells were washed with RPMI
336 1640 media three times to remove the free proteins. Then cells were collected by cell scrapers,

centrifuged at 600 rpm for 5 min and resuspended in PBS. After washes twice with PBS and centrifugation at 600 rpm for 5 min, cells were fixed by adding 1 ml of 1% paraformaldehyde-PBS. Following washes twice with PBS, the cells were incubated with anti-Rv3194c antibody (1:100) for 2 h. After incubation with primary antibody, cells were washed with PBS for three times and incubated with goat anti-rabbit IgG conjugated with Alexa Fluor 488 (1:10000) for 1h. The cells were analyzed by confocal microscopy and flow cytometry using Cellquest™ software (BD Biosciences, San Jose, CA, USA).

Experimental Infection in Vitro

Rv3194c/MS was prepared as described above. The Rv3194c/MS were harvested in 7H9 broth at 37 °C until the cells reached an OD_{650} of 0.6. The bacterial suspension was prepared by the conventional method (32). A549 cells were treated with 100 μg/mL of HA or P91-110 dissolved in binding medium (138 mM NaCl, 8.1 mM Na_2HPO_4, 1.5 mM KH_2PO_4, 2.7 mM KCl, 0.6 mM $CaCl_2$, 1 mM $MgCl_2$, and 5.5 mM D-glucose) for 2 h. Rv3194c/MS at an MOI of 10:1 was subsequently added to these treated cells or untreated cells. After infection with Rv3194c/MS, the cells were washed three times with RPMI 1640 media, scraped with a rubber policeman and centrifuged. The pellet was then resuspended in 7H9 broth, and the cell suspension were grown on 7H10 agar plates. The colonies were incubated at 37ºC for three days and then counted. Confocal microscopy and flow cytometry was used to assess the association of Rv3194c/MS with A549 cells as described in the methods for the protein binding assay.

Experimental Infection in Vivo

Barrier-bred female 6-12 week BALB/c mice used for the lung infection assays were

obtained from the Shanghai Laboratory Animal Center, Chinese Academy of Science (SLACCAS), maintained in specific pathogen-free (SPF) conditions. After the mice were randomly divided into four groups, they were anaesthetized with dry ice before the bacteria were infected. The10^7 CFUs of rMS (Rv3194c+FFlucRT/MS, FFlucRT/MS) were inoculated the mice by nasal administration. In addition, the 10^7 CFUs of Rv3194c+FFlucRT/MS were mixed with100 μg of HA or P91-110, and the mixture was also inoculated other mice by nasal administration. At 1, 4, 7 and 14 days post infection, bioluminescence imaging and bacterial counts in the lung tissue were performed to track the disease progression. The bioluminescence [photons/s/cm^2/steradian (sr)] was assessed from the living animals using an IVISw Spectrum system. The mice were intraperitoneally injected with 500 mg/kg body weight of D-luciferin dissolved in sterile D-PBS containing ketamine before the bioluminescent imaging. The mice were confined to a large airtight box to ensure safe conditions and placed into the imaging chamber of the IVISw Spectrum imaging system with the stage that had been heated to 37 °C. The bioluminescence within specific regions of the individual mice was also quantified by the ROI tool in the Living Image software program (set as photons/s). The *in vivo* imaging was immediately performed at specific time points. The animals were culled while still under anesthesia by cervical dislocation, and the lungs were aseptically removed. The entire left lobe of the lung was homogenized with a set of motor and pestle, and then was plated on 7H10 agar plates with 50 μg/mL kanamycin. After 3 days of incubation at 37 °C, the CFU of the rMs was calculated.

Statistical analysis

Each experiment was repeated in triplicate. A two-tailed Student's t test was used to determine the statistical significance, and Prism software (version 5.0; GraphPad, San Diego, CA, USA) was used for these analyses. Data that appeared to be statistically significant were analyzed using an analysis of variance (ANOVA) to compare the means of multiple groups. The means were considered to be significant if the P values were less than 0.05 ($0.01 < {}^{*}P < 0.05$, ${}^{**}P < 0.01$ and ${}^{***}P < 0.001$).

Acknowledgments

This study was supported by the National Natural Science Foundation of China (No. 31901930), Educational Department Project (Category A) of Fujian Province (No. JT180080) and the scientific research innovation program "Xiyuanjiang River Scholarship" of College of Life Sciences of Fujian Normal University.

Conflict of interest

The authors declare that the research was conducted in the absence of any commercial or financial relationships that could be construed as a potential conflict of interest.

Author contributions

D.Z., C.X. and D.L. conceived and designed the experiments, analyzed the data. D.Z., C.X. and D.L. performed the experiments. D.Z. wrote the manuscript.

Ethical approval

The animal use protocol listed has been reviewed and approved by the Animal Ethical and Welfare Committee (AEWC) of Fujian Normal University (FJNU) (No. of Animal use permit:

SYXK: 2015-0004, Approval No. IACUC-20190033).

Data availability statement:

All data generated or analyzed during this study are included in this article.

References

1. Bloom BR, Salomon JA. 2005. Enlightened self-interest and the control of tuberculosis. N Engl J Med 353:1057-1059.
2. Smith I. 2003. *Mycobacterium tuberculosis* pathogenesis and molecular determinants of virulence. Clin Microbiol Rev 16:463-496.
3. Krachler AM, Orth K. 2013. Made to stick: anti-adhesion therapy for bacterial infections. Microbe 8:286-290.
4. Stones DH, Krachler AM. 2015. Fatal attraction: how bacterial adhesins affect host signaling and what we can learn from them. Int J Mol Sci 16:2626-2640.
5. Ribet D, Cossart P. 2015. How bacterial pathogens colonize their hosts and invade deeper tissues. Microbes Infect 17:173-183.
6. Ramsugit S, Pillay M. 2015. Pili of *Mycobacterium tuberculosis*: current knowledge and future prospects. Arch Microbiol 197:737-744.
7. Asadi A, Razavi S, Talebi M, Gholami M. 2019. A review on anti-adhesion therapies of bacterial diseases. Infection 47:13-23.
8. Mehta PK, Karls RK, White EH, Ades EW, Quinn FD. 2006. Entry and intracellular replication of Mycobacterium tuberculosis in cultured human microvascular endothelial cells.

421 Microb Pathog 41:119-124.

422 9. Ramsugit S, Pillay M. 2014. *Mycobacterium tuberculosis* pili promote adhesion to and
423 invasion of THP-1 macrophages. Jpn J Infect Dis 67:476-478.

424 10. Brennan MJ, Delogu G, Chen Y, Bardarov S, Kriakov J, Alavi M, Jacobs WR. 2001.
425 Evidence that mycobacterial PE-PGRS proteins are cell surface constituents that influence
426 interactions with other cells. Infect Immun 69:7326-7333.

427 11. Ramsugit S, Pillay B, Pillay M. 2016. Evaluation of the role of *Mycobacterium tuberculosis*
428 pili (MTP) as an adhesin, invasin, and cytokine inducer of epithelial cells. Braz J Infect Dis
429 20:160-165.

430 12. Hickey TB, Thorson LM, Speert DP, Daffé M, Stokes RW. 2009. *Mycobacterium*
431 *tuberculosis* Cpn60.2 and DnaK are located on the bacterial surface, where Cpn60.2
432 facilitates efficient bacterial association with macrophages. Infect Immun 77:3389-3401.

433 13. Kumar S, Puniya BL, Parween S, Nahar P, Ramachandran S. 2013. Identification of novel
434 adhesins of *M. tuberculosis* H37Rv using integrated approach of multiple computational
435 algorithms and experimental analysis. PLoS One 8:e69790.

436 14. Pethe K, Puech V, Daffé M, Josenhans C, Drobecq H, Locht C, Menozzi FD. 2001.
437 *Mycobacterium smegmatis* laminin-binding glycoprotein shares epitopes with
438 *Mycobacterium tuberculosis* heparin-binding haemagglutinin. Mol Microbiol 39:89-99.

439 15. Kinhikar AG, Vargas D, Li H, Mahaffey SB, Hinds L, Belisle JT, Laal S. 2006.
440 *Mycobacterium tuberculosis* malate synthase is a laminin-binding adhesin. Mol Microbiol
441 60:999-1013.

16. Espitia C, Laclette JP, Mondragón-Palomino M, Amador A, Campuzano J, Martens A, Singh M, Cicero R, Zhang Y, Moreno C. 1999. The PE-PGRS glycine-rich proteins of *Mycobacterium tuberculosis*: a new family of fibronectin- binding proteins? Microbiology 145:3487-3495.

17. Xolalpa W, Vallecillo AJ, Lara M, Mendoza-Hernandez G, Comini M, Spallek R, Singh M, Espitia C. 2007. Identification of novel bacterial plasminogen-binding proteins in the human pathogen *Mycobacterium tuberculosis*. Proteomics 7:3332-3341.

18. Esparza M, Palomares B, García T, Espinosa P, Zenteno E, Mancilla R. 2015. PstS-1, the 38-kDa *Mycobacterium tuberculosis* glycoprotein, is an adhesin, which binds the macrophage mannose receptor and promotes phagocytosis. Scand J Immunol 81:46-55.

19. Diaz-Silvestre H, Espinosa-Cueto P, Sanchez-Gonzalez A, Pereira-Suarez AL, Bernal-Fernandez G, Espitia C, Mancilla R. 2005. The 19-kDa antigen of *Mycobacterium tuberculosis* is a major adhesin that binds the mannose receptor of THP-1 monocytic cells and promotes phagocytosis of mycobacteria. Microb Pathog 39:97-107.

20. Aoki K, Matsumoto S, Hirayama Y, Wada T, Ozeki Y, Niki M, Domenech P, Umemori K, Yamamoto S, Mineda A, Matsumoto M, Kobayashi K. 2004. Extracellular mycobacterial DNA-binding protein 1 participates in mycobacterium-lung epithelial cell interaction through hyaluronic acid. J Biol Chem 279:39798-397806.

21. Menozzi FD, Rouse JH, Alavi M, Laude-Sharp M, Muller J, Bischoff R, Brennan MJ, Locht C. 1996. Identification of a heparin-binding hemagglutinin present in mycobacteria. J Exp Med 184:993-1001.

22. Russell DG. 2011. *Mycobacterium tuberculosis* and the intimate discourse of a chronic infection. Immunol Rev 240:252-268.

23. Yang B, Yang BL, Savani RC, Turley EA. 1994. Identification of a common hyaluronan binding motif in the hyaluronan binding proteins RHAMM, CD44 and link protein. EMBO J 13:286-296.

24. Li H, Dang G, Liu H, Wang Z, Cui Z, Song N, Chen L, Liu S. 2019. Characterization of a novel *Mycobacterium tuberculosis* serine protease (Rv3194c) activity and pathogenicity. Tuberculosis 119:101880.

25. Liu PT, Modlin RL. 2008. Human macrophage host defense against *Mycobacterium tuberculosis*. Curr Opin Immunol 20:371-376.

26. Chaudhuri R, Kulshreshtha D, Raghunandanan MV, Ramachandran S. 2014. Integrative immunoinformatics for *Mycobacterial* diseases in R platform. Syst Synth Biol 8:27-39.

27. Ramsugit S, Pillay M. 2016. Identification of *Mycobacterium tuberculosis* adherence-mediating components: a review of key methods to confirm adhesin function. Iran J Basic Med Sci 19:579-584.

28. Dang G, Cao J, Cui Y, Song N, Chen L, Pang H, Liu S. 2016. Characterization of Rv0888, a novel extracellular nuclease from *Mycobacterium tuberculosis*. Sci Rep 6:19033.

29. Yuan X, Chen L, Deng X, Cao J, Yu S, Quankai W, Pang H, Liu S. 2013. Characterization of Rv0394c gene encoding hyaluronidase and chondrosulfatase from *Mycobacterium tuberculosis*. Tuberculosis 93:296-300.

30. Vizcaíno C, Patarroyo ME, Patarroyo MA. 2010. Computational prediction and

experimental assessment of secreted/surface proteins from *Mycobacterium tuberculosis* H37Rv. PLoS Comput Biol 6:e1000824.

31. Matsumoto S, Yukitake H, Furugen M, Matsuo T, Mineta T, Yamada T. 1999. Identification of a novel DNA-binding protein from *Mycobacterium bovis* bacillus Calmette-Guérin. Microbiol Immunol 43:1027-1036.

32. Hoal-van Helden EG, Hon D, Lewis LA, Beyers N, van Helden PD. 2001. Mycobacterial growth in human macrophages: variation according to donor, inoculum and bacterial strain. Cell Biol Int 25:71-81.

492 **Figure captions**

493 **FIG 1 Expression, purification and validation of the Rv3194c protein. A**, Analysis of
494 Rv3194c protein by SDS-PAGE. Lane 1, the supernatant of induced cells after disruption; Lane 2,
495 agarose resin after supernatant to pass through column; Lane 3, agarose resin after column
496 washed by wash buffer; Lane 4, purified Rv3194c protein was eluted by 20 mM Tris, 200 mM
497 imidazole and 150 mM NaCl, (pH 7.5); Lane 5, purified Rv3194c protein was eluted using 20
498 mM Tris, 500 mM imidazole and 150 mM NaCl, (pH 7.5). **B**, Analysis of Rv3194c protein by
499 western blotting. Lane 1, pET28a-Rv3194c without induction served as a negative control; Lane
500 2, pET28a-Rv3194c with induction; Lane 3, the cell lysate of BCG served as a positive control.
501 **C,** Gel filtration chromatography of the Rv3194c protein. Proteins collected in different tube
502 from 6 to10 were respectively detected by SDS-PAGE. D MALDI-TOF peptide mass fingerprint
503 spectrometry for the recombinant Rv3194c. The sequence of Rv3194c covering these fragments
504 is displayed as bolded in red.

505 **FIG 2 Rv3194c binds to HA**. **A,** The content of Rv3194c in the immobilized wells was tested
506 by ELISA. Rv3295 instead of Rv3194c served as a negative control. **B,** Analysis of HA-binding
507 proteins using HA-Sepharose chromatography. T, total Rv3194c protein applied to
508 chromatography; F, flow-through; Lane1-6, Rv3194c eluted by 1.5M NaCl. **C,** The
509 Rv3194c-specific HA binding region was determined by ELISA. 20-mer of sequential peptides
510 corresponding to the amino acid sequence of Rv3194c was synthesized. *OD*, optical density; *NC*,
511 negative control without peptide.

512 **FIG 3 The interaction of Rv3194c/P91-110 with HA analyzed by surface plasmon resonance.**

513 Results for Rv3194c (**A**) and P91-110 (**B**) are shown. Injections of different concentrations of
514 HA flowed over a surface chip at a flow rate of 10 μL/min. Concentration of the analyte: 15, 30,
515 60, 120 and 240 nM.

516 **FIG 4 Rv3194c binds to A549 human lung epithelial cells. A**, The binding of Rv3194c (**a**) and
517 Cy3-P91-110 (**b**) to A549 cells was visualized by confocal microscope. Magnification fold
518 (600×). **B**, Binding kinetics of Cy3-P91-110 and Rv3194c to the A549 cells. Cy3-P91-110-bound
519 cells and Rv3194c-bound cells were identified using FACScan at each time point (30, 60, 90,
520 120 min). **C**, The percentage of Rv3194c-bound A549 cells were identified by FACScan.
521 Untreated A549 cells bound to Rv3295 as negative control (**a**) and to Rv3194c (**b**). Rv3194c was
522 added to the culture of cells pretreated with hyaluronidase (**c**), HA (**d)** and P91-110 (**e**).

523 **FIG 5 Rv3194c is involved in the recombinant *M. smegmatis* process of attachment and**
524 **binding to the A549 cells. A**, The attachment of the Rv3194c/MS (**a**) and pMV261/MS (**b**) to
525 the A549 cells was visualized by confocal microscope. pMV261/MS served as a negative control.
526 **B**: The binding was measured using bacterial count. Untreated A549 cells were infected with
527 pMV261/MS as negative control and with Rv3194c/MS. Rv3194c/MS was added to the culture
528 of cells pretreated with P91-110 and HA. **C**, Subcellular localization of Rv3194c in Rv3194c/MS
529 was detected by western blotting. Lanes: 1, cell wall; 2, cell membrane; 3, whole-cell lysates; 4,
530 cytoplasm; 5, cell culture filtrates. KatG protein serves as a cytoplasm marker.

531 **FIG 6 Inhibition of the infection of *in vivo* recombinant *M. smegmatis*. A**, Construction of the
532 FFlucRT reporter plasmids and strains. **A**, *Rv3194c* and *FFlucRT* containing the G13 promoter
533 were respectively cloned into the *E. coli-mycobacterium* shuttle vector pMV261 at the *Bst*B

534 I-*Hind III* and the *Hind III-Sal* I sites. **B and C**, Bacterial loads (**B**) and bioluminescence **(C)** in
535 infected lung tissue from BALB/c mice. The mice was infected with FFlucRT/MS as a negative
536 control (**a**), with Rv3194c+FFlucRT/MS (**b**), with Rv3194c+FFlucRT/MS plus of P91-110 (**c**)
537 and with Rv3194c+FFlucRT/MS plus of HA (**d**) by nasal administration. Bckg, background
538 luminescence (1.0×10^4 photons/s).

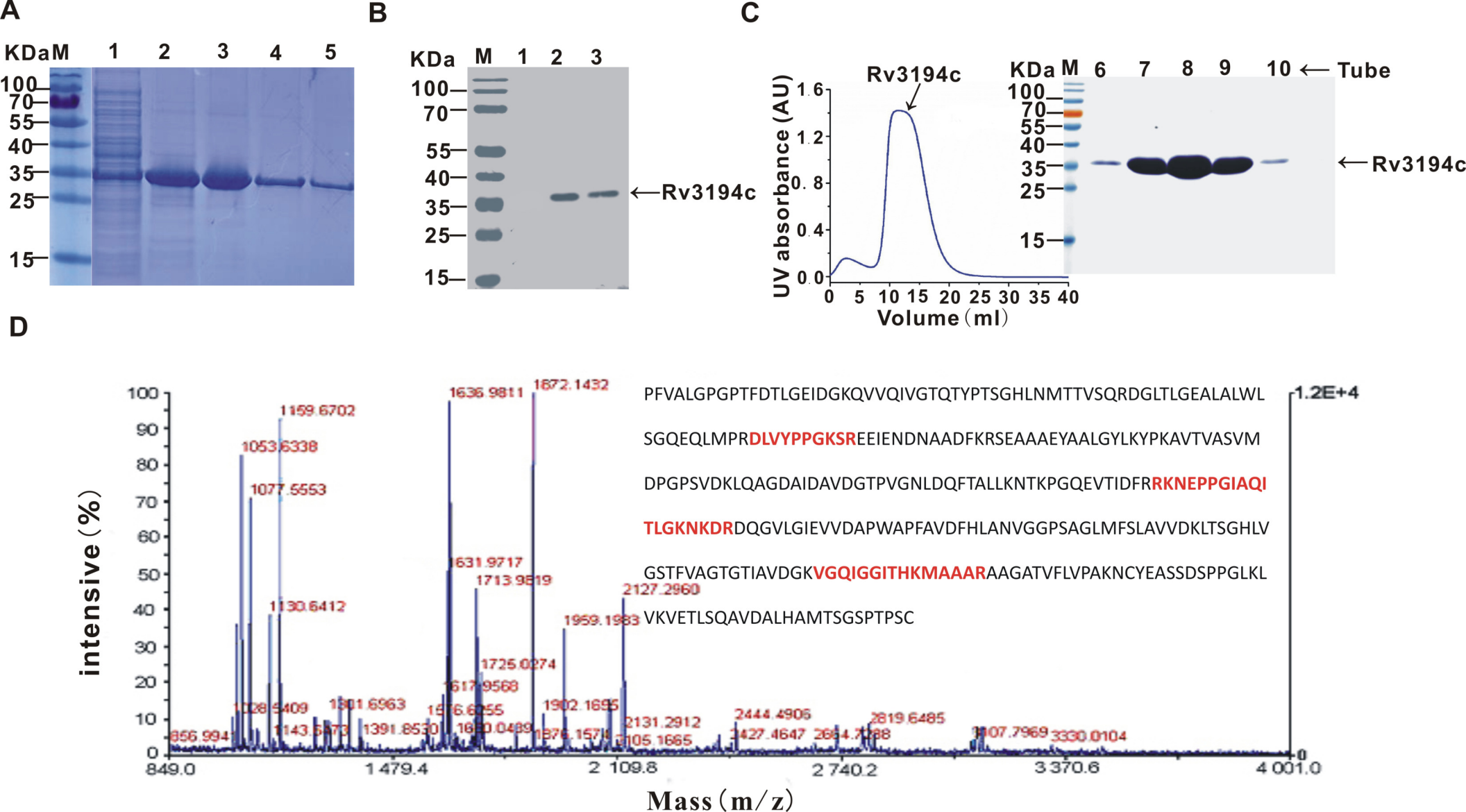
A
KDa M 1 2 3 4 5
100
70
55
40
35
25
15
B
KDa M 1 2 3
100
70
55
40
35
25
15
Rv3194c
C
Rv3194c
UV absorbance (AU)
Volume (ml)
KDa M 6 7 8 9 10
Tube
Rv3194c
D
intensive (%)
Mass (m/z)
PFVALGPGPTFDTLGEIDGKQVVQIVGTQTYPTSGHLNMTTVSQRDGLTLGEALALWL
SGQEQLMPRDLVYPPGKSREEIENDNAADFKRSEAAAEYAALGYLKYPKAVTVASVM
DPGPSVDKLQAGDAIDAVDGTPVGNLDQFTALLKNTKPGQEVTIDFRRKNEPPGIAQI
TLGKNKDRDQGVLGIEVVDAPWAPFAVDFHLANVGGPSAGLMFSLAVVDKLTSGHLV
GSTFVAGTGTIAVDGKVGQIGGITHKMAAARAAGATVFLVPAKNCYEASSDSPPGLKL
VKVETLSQAVDALHAMTSGSPTPSC

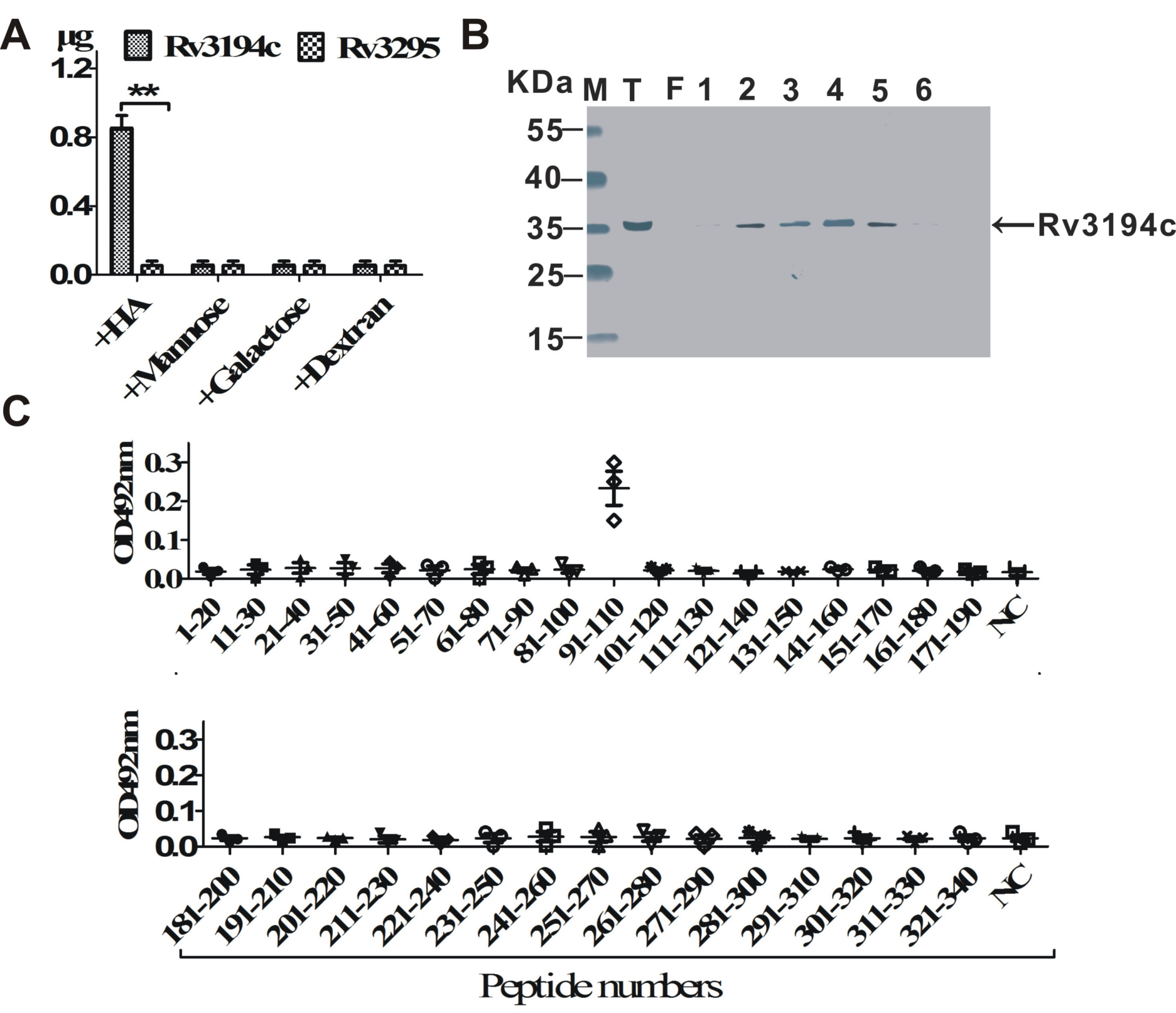
A
μg
Rv3194c
Rv3295
1.2
0.8
0.4
0.0
**
+HA
+Mannose
+Galactose
+Dextran
B
KDa
M T F 1 2 3 4 5 6
55
40
35
25
15
Rv3194c
C
OD492nm
0.3
0.2
0.1
0.0
1-20
11-30
21-40
31-50
41-60
51-70
61-80
71-90
81-100
91-110
101-120
111-130
121-140
131-150
141-160
151-170
161-180
171-190
NC
181-200
191-210
201-220
211-230
221-240
231-250
241-260
251-270
261-280
271-290
281-300
291-310
301-320
311-330
321-340
Peptide numbers

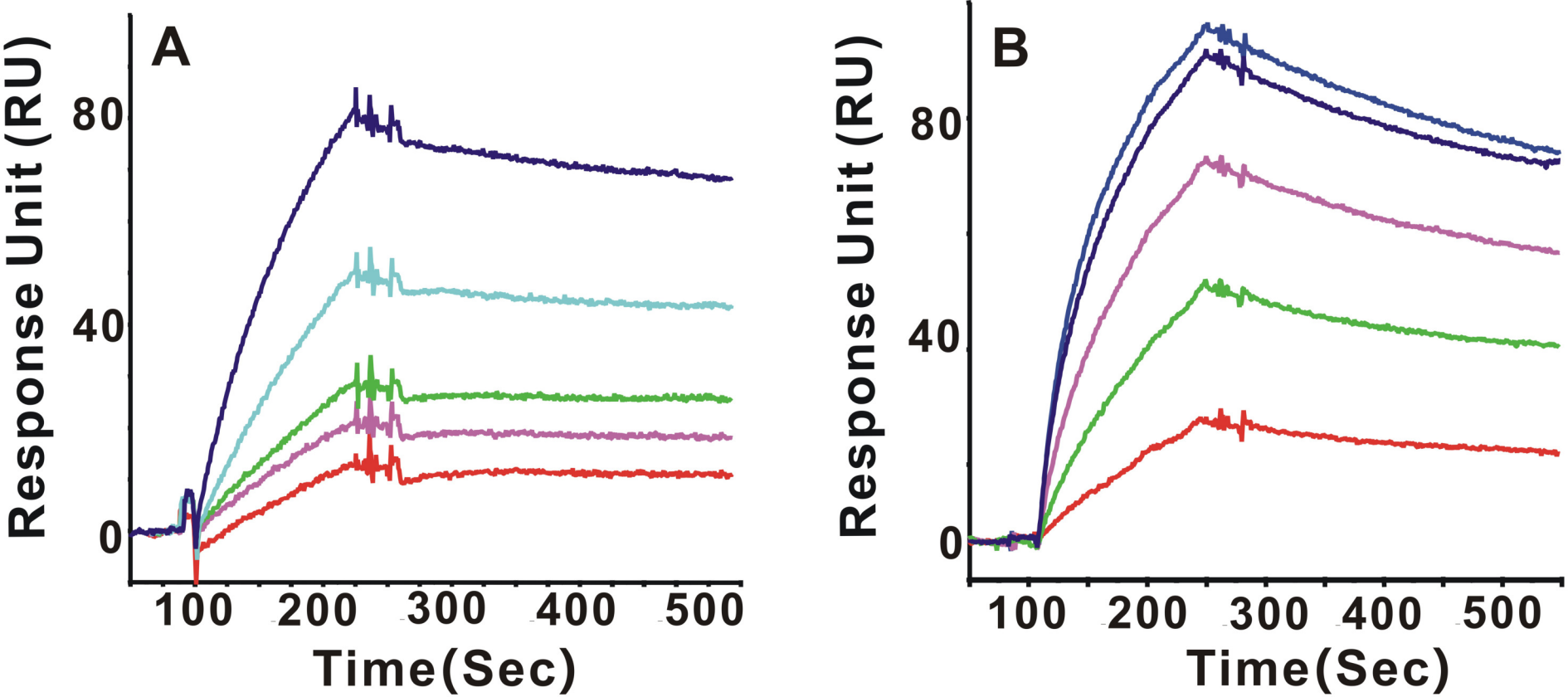

Table 1

Kinetics parameters for Rv3194c/P91-110-HA interaction from *SPR* analysis

Immobilized ligand	Analytes	Association rate, k_a	Dissociation rate, k_d	Affinity, K_D
		$L \cdot mol^{-1} \cdot s^{-1}$	S^{-1}	mol/L
Rv3194c	HA	2×10^{4}	5×10^{-4}	2×10^{-8}
P91-110	HA	3×10^{3}	4×10^{-5}	1.6×10^{-8}

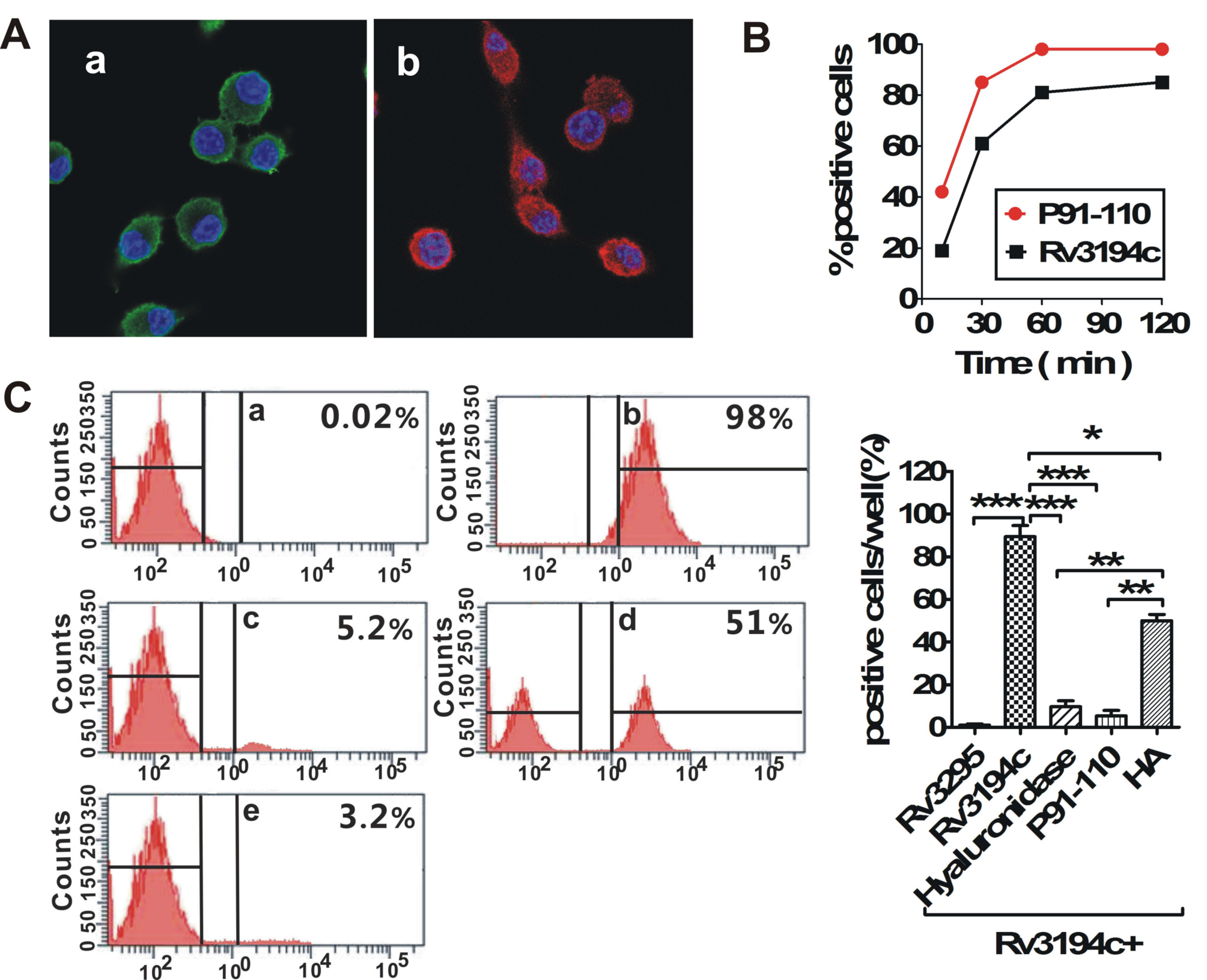
A
a
b
B
%positive cells
100
80
60
40
20
0
0
30
60
90
120
Time (min)
P91-110
Rv3194c
C
Counts
a
0.02%
b
98%
c
5.2%
d
51%
e
3.2%
positive cells/well(%)
120
100
80
60
40
20
0
Rv3295
Rv3194c
Hyaluronidase
P91-110
HA
Rv3194c+
*
***
***
***
**
**

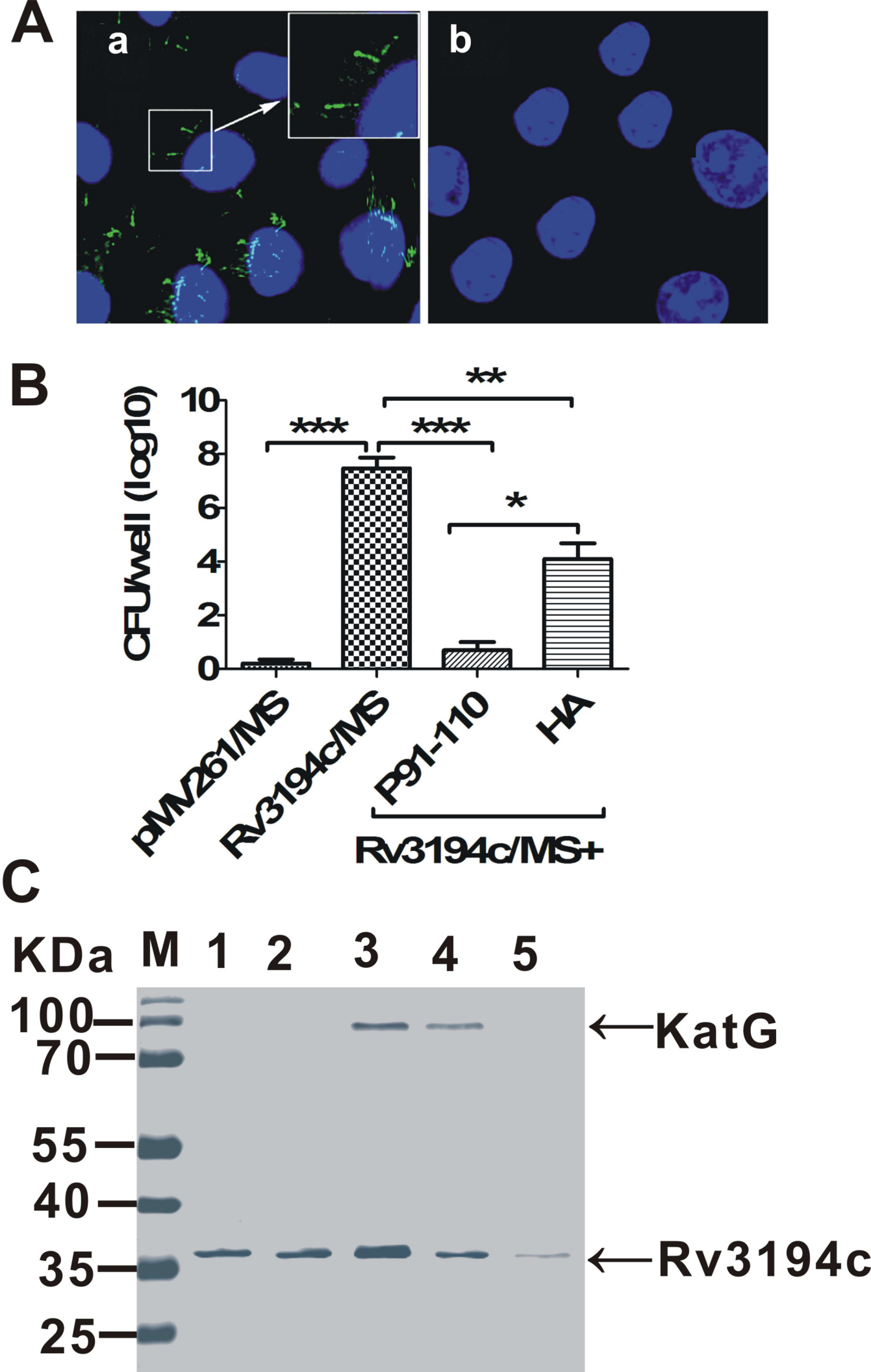
A
a
b
B
CFU/well (log10)
10
8
6
4
2
0
***
***
**
*
pMV261/MS
Rv3194c/MS
P91-110
HA
Rv3194c/MS+
C
KDa
M
1
2
3
4
5
100
70
55
40
35
25
KatG
Rv3194c

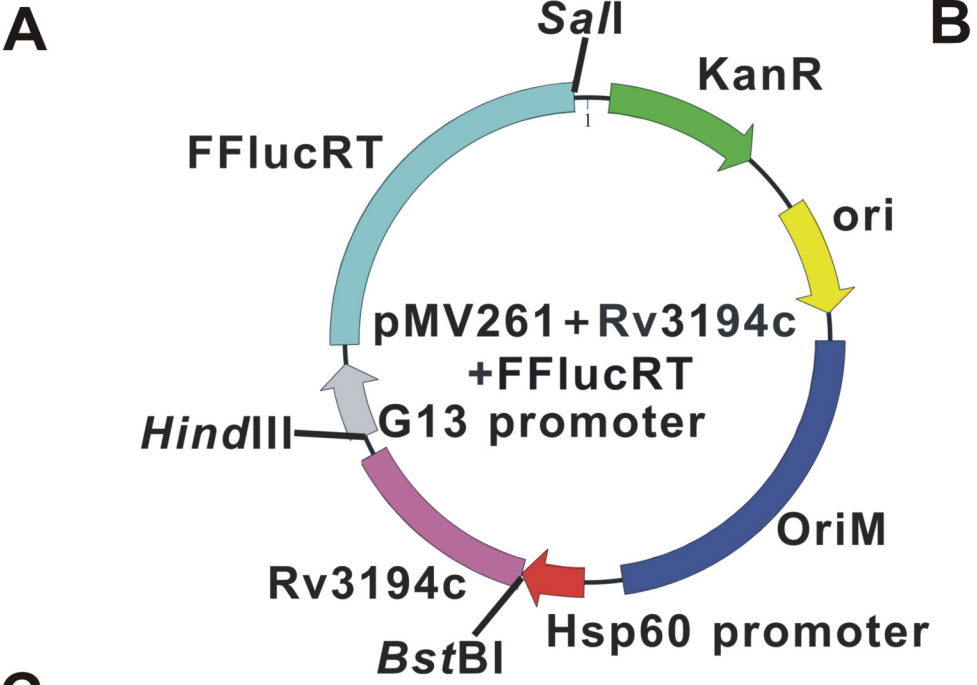
A
SalI
KanR
FFlucRT
ori
pMV261+Rv3194c
+FFlucRT
G13 promoter
HindIII
OriM
Rv3194c
Hsp60 promoter
BstBI

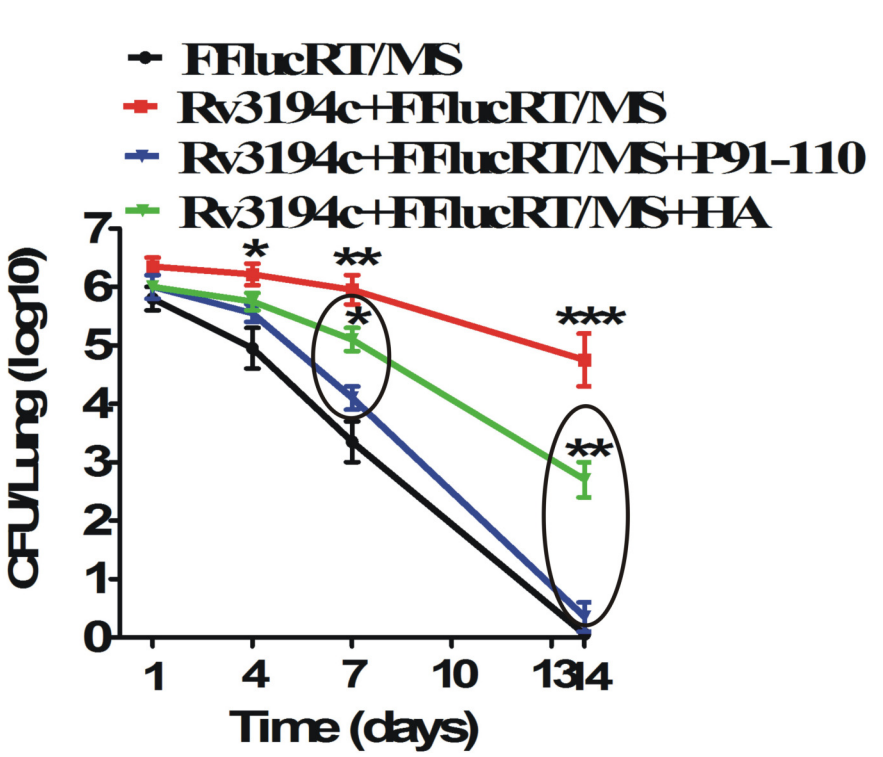
B
FFlucRT/MS
Rv3194c+FFlucRT/MS
Rv3194c+FFlucRT/MS+P91-110
Rv3194c+FFlucRT/MS+HA
CFU/Lung (log10)
Time (days)

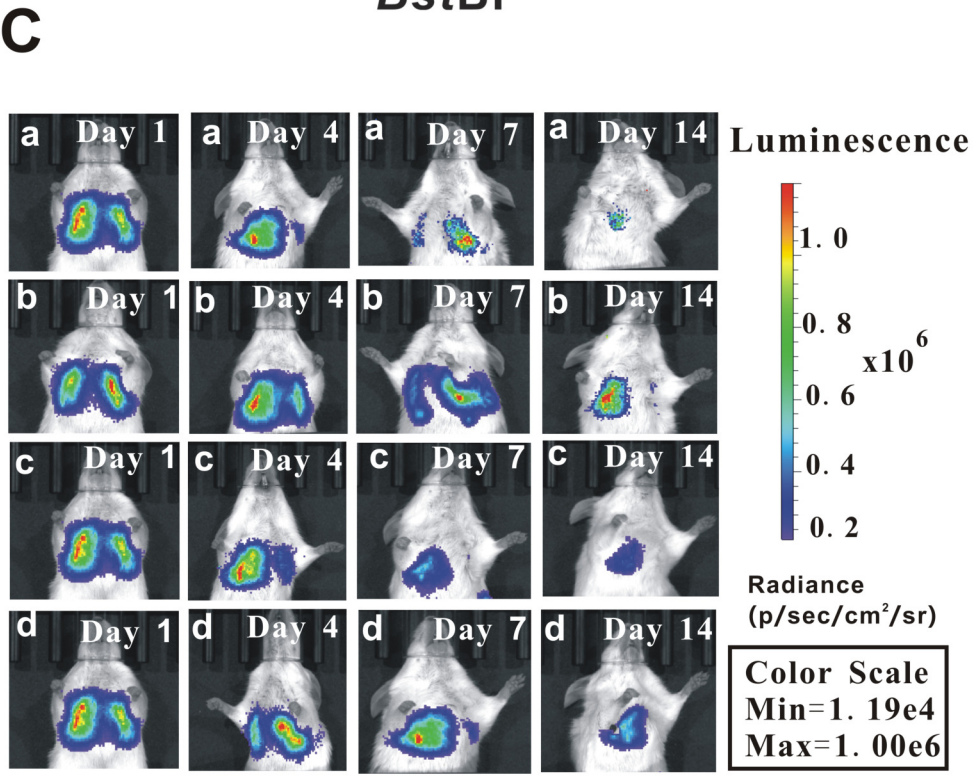
C
Day 1
Day 4
Day 7
Day 14
Luminescence
x10^6
Radiance
(p/sec/cm²/sr)
Color Scale
Min=1. 19e4
Max=1. 00e6

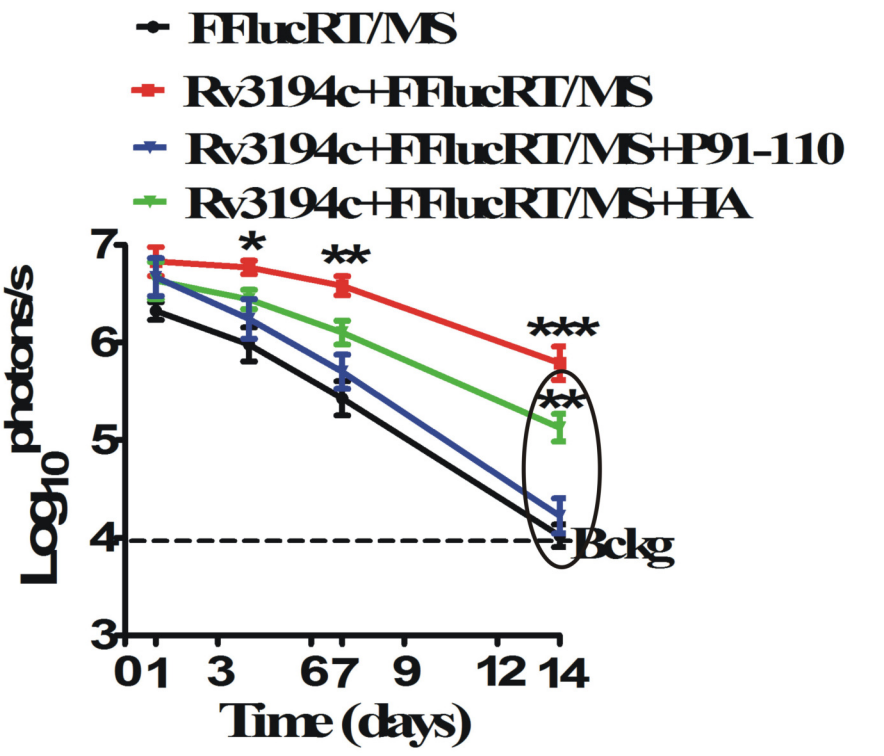
FFlucRT/MS
Rv3194c+FFlucRT/MS
Rv3194c+FFlucRT/MS+P91-110
Rv3194c+FFlucRT/MS+HA
Log10 photons/s
Bckg
Time (days)